

# Ring Bank Theory: Insights into Consciousness from Observed Geometry and Neural Dynamics of Hyperpolarization

Brad Caldwell, BSCE  
caldwbr@gmail.com

October 25, 2025

## Abstract

**Ring Bank Theory** (RBT) presents a geometric framework for consciousness centered on rhythmic access to spatial representation. The theory proposes three core components: a persistent 3D spatial scaffold (**Bank**) maintaining perspective-invariant relations, dynamic sampling patterns (**Union Set**) operating across continuous-to-discrete modes, and a temporal integration system (**Time Schema**). Conscious representation follows a strict **when** → **where** → **what** hierarchy, where temporal indexing precedes content binding. A high-level **microphone signal** competes with a wandering **baseline rhythm** to trigger/modulate union set behavior, initiating a **cascading semiotic process** from perceptual signals to behavioral outputs. This geometric framework provides a rendering solution to the binding problem, proposes a mechanism for dissociation phenomena through temporary **phasic anticorrelation** of brain regions when entrained at a slow rhythm, and generates testable predictions about the neural dynamics of conscious representation, particularly in **hyperpolarization**.

## 1 Core Architecture

### 1.1 Bank Schema (Shape Schema): 3D Content-Shaped Manifestation

The bank  $\mathcal{B}$  potentially correlates with the concentric sphere/cube/cylinder shells following shock scaffolds as mentioned by Steven Lehar [9], and manifests with display scale, rotation, and location shaped by content (preconscious and postconscious):

$$\mathcal{B} \equiv \left\{ \mathbf{x} \in \mathbb{R}^3 \mid \frac{\|\mathbf{x}_i - \mathbf{x}_j\|}{\|\mathbf{x}_k - \mathbf{x}_l\|} = C_{ijkl} \right\} \quad (1)$$

where unconscious content  $C_u$  influences display properties  $\mathbf{D} = (S_d, \mathbf{R}_d, \mathbf{T}_d)$  and conscious deduction and attention drive convergence:

$$\mathbf{D} \rightarrow \mathbf{D}_{\text{semantic}}(C) \quad \text{as} \quad C_u \rightarrow C \quad (2)$$

### 1.2 Real Schema: 3D Veridical World Model for Action

The real schema  $\mathcal{R}$  is the 3D understanding of the immediate world that guides the body schema and physical movement. It consists of:

- **Stereo geometry:** Left-eye and right-eye volumes merged into a cyclopean view behind the nose via rotation around the focal object,
- **Hierarchical structure:** Nested schemas including body, environment, and key object representations,

- **Dual temporal modes:** Both static (present snapshot) and dynamic (changing world) representations.

As the servo target for physical action,  $\mathcal{R}$  provides the spatial framework for avatar movement and real-world interaction. Movement errors often arise from **attitude misalignment** between the **body schema** and the visually-derived **environment schema** (the two main components of  $\mathcal{R}$ ). For example, a **yaw error** in the body schema—where it is assumed to be rotated slightly clockwise (bird’s-eye view) from its actual position relative to the visually perceived refrigerator—results in an underreach when grasping the handle. The arm is miscalculated as being closer to the target than it actually is, despite correct trajectory planning.

### 1.3 Imaginal Schema: 3D Non-Veridical Geometric Workspace

The imaginal schema  $\mathcal{I}$  provides a dynamic volumetric overlay to the real schema  $\mathcal{R}$ , serving as a workspace for non-veridical spatial representation and reasoning. Key properties include:

- **Functional scope:** Generates hypothetical situations, warning imagery (e.g., potential bitten-finger flash when bringing fingers into mouth while eating chips to induce caution), memories, conceptual contemplation, action simulations, and dream content,
- **Viewing perspective:** Typically observed by a “mind’s eye” that can orbit, relocate, or rapidly zoom independently of the avatar’s cyclopean eye in  $\mathcal{R}$ , though dreams and certain cases may embed a “mind’s avatar” within  $\mathcal{I}$ ,
- **Dynamic interaction:** Frequent switching between  $\mathcal{R}$  and  $\mathcal{I}$  occurs during normal cognition, with  $\mathcal{I}$  serving as a temporary workspace before returning to reality-based processing,
- **Display dominance:** While often overlaying  $\mathcal{R}$ ,  $\mathcal{I}$  can fully dominate conscious frames, creating anticorrelated periods of purely imaginal or real experience,
- **Volumetric scaling:** Objects are dynamically rescaled relative to  $\mathcal{R}$  with extreme rapidity—comparable to the fastest camera zoom—frequently enlarging small elements for detailed inspection,
- **Variable visibility:** Ranges from completely transparent to vivid and photorealistic, with individual differences in conscious access—some experience  $\mathcal{I}$  as plain as day while others have little visual awareness,
- **Non-veridical content:** Supports imagined, remembered, or potential future geometries—places, times, and scenarios not matching to  $\mathcal{R}$ ,
- **Geometric utility:** Maintains full spatial functionality regardless of visibility, enabling both conscious inspection and “blindsight”-style geometric processing.

Unlike the action-oriented  $\mathcal{R}$ ,  $\mathcal{I}$  serves as a flexible workspace where metacognition operates as observer of non-literal geometric content. It is possible to have more than one  $\mathcal{I}$  at once.

### 1.4 Time Schema: 3D Temporal Flow or Time Window

The time schema  $\mathcal{T}$  provides the temporal architecture for conscious experience, organizing perception into a flowing sequence of discrete moments. Typically, a plane is devoted as an embedding location for  $\mathcal{U}$ , and the axis **normal** to this plane flows and fades “that-printed” over a period such as one second. Key properties include:

- **Ringframe sequencing:** Maintains a fading history of recent perceptual moments printed from the Union Set, creating temporal continuity,

- **Multi-modal operation:** Supports both continuous phasic scanning and discrete interrupt sampling through the  $\tau \leq T$  relationship,
- **Dynamic timing:** Governs sampling frequency through competition between wandering baseline rhythm  $\beta(t)$  and event-driven interrupts,
- **Temporal integration:** Provides the weighted history window for content determination in  $\mathcal{R}$  and  $\mathcal{I}$  schemas,
- **Flow illusion:** Generates the experience of continuous awareness through rhythmic, discrete sampling of spatial representations.

As the temporal container for consciousness,  $\mathcal{T}$  transforms spatial representations in  $\mathcal{B}$ ,  $\mathcal{R}$ , and  $\mathcal{I}$ , mainly as sampled at 0–2D ringframes, into the stream of lived experience.

### 1.5 Union Set: 0–2D Manifold Access Gradient

Any given instantiation of union set  $\mathcal{U}$  has an infinitesimal life, immediately decaying to mere **ringframe** material and then flowing and fading away in the time schema  $\mathcal{T}$ . The high-level **microphone signal**  $\mathcal{M}$  and **baseline rhythm**  $\beta(t)$  modulate the ongoing behavior of the Union Set  $\mathcal{U}$ . Filtered or crafted stimulus events and baseline rhythms first instantiate—and timestamp themselves—on the shared manifold  $\mathcal{U}$ . From this primary interface, the Real and Imaginal schemas  $[\mathcal{R}, \mathcal{I}]$  must subsequently render, often with additional latency, while ringframes flow away and fade within the Time Schema  $\mathcal{T}$ .

The following equations approximate the dynamic behavior of  $\mathcal{U}$ , which is governed by baseline rhythms and external events.  $\mathcal{U}$  frequently exhibits intra-bin spatial cyclism, revolving or orbiting (the Ring Cycle) with a period  $\tau$  that is less than or equal to the Bin Cycle  $T$ .

$$\text{Ring Cycle } (0 \rightarrow 2\pi) \tau \leq \text{Bin Cycle } (0 \rightarrow 0) T : \quad (3)$$

$$\text{3D Spirographic } (\tau = T) : \gamma_{2D}(t) = \{\mathbf{x} : \|\mathbf{x} - \mathbf{c}(t)\| = R\}, \quad \mathbf{c}(t) = R_s(\cos \omega_s t, \sin \omega_s t, 0) \quad (4)$$

$$\text{Phasic } (\tau = T) : \gamma(t) = \mathbf{p}(\phi(t) \text{ or } s(t)), \quad \phi(T) = 2\pi, \quad s(T) = L, \quad \dot{\phi} = \omega \text{ or } \dot{s} = v \quad (5)$$

$$\text{Discontinuous } (\tau < T) : \gamma(t) = \mathbf{p}(\phi(t) \text{ or } s(t)) \text{ for } t \in [kT, kT + \tau], \quad \phi(\tau) = 2\pi, \quad s(\tau) = L \quad (6)$$

$$\text{Interrupt } (\tau \rightarrow 0) : \Sigma_k = \{\mathbf{x} \mid f_k(\mathbf{x}) = 0\} \quad (7)$$

$$\text{with Bin Trigger: } t_{\text{next}} = \min \left( t_{\text{last}} + \beta(t)^{-1}, \min_i \{t_i \mid \alpha_i > \theta(I_{\text{last}}, t - t_{\text{last}})\} \right) \quad (8)$$

$$\text{where } \theta(I, \Delta t) = \theta_\infty + I \cdot e^{-\Delta t / \tau_r}, \quad \beta(t) \in [\beta_{\min}, \beta_{\max}] \quad (9)$$

#### Union Set Access Description:

The Union Set displays various modes of sampling  $[\mathcal{B}, \mathcal{R}, \mathcal{I}]$  and printing into  $\mathcal{T}$ :

- **3D spirographic mode:** A 2D shell rotor (sphere, cylinder, etc.) remains hot (active) while moving spirographically (the center follows a circular trajectory),
- **Phasic mode:** A tracer moves continuously along a path. In this continuous mode, the baseline rhythm does not induce a refractory period, and sampling is sustained,
- **Event-driven modulation:** In continuous modes (e.g., Phasic), the amplitude envelope of the microphone signal  $\mathcal{M}$  can perturb the tracer’s trajectory in real-time, warping the ring path instead of triggering discrete interrupts,
- **Discontinuous mode:** The tracer completes the same 0–2pi period ( $\tau$ ) path in less than the cycle period ( $T$ ), leaving a silent gap before the next ringframe,

- **Interrupt mode:** Instantaneous sampling of geometric shapes occurs at discrete times with near-zero active duration,
- **Bin Triggering:** The timing of sampling in interrupt mode is determined by either:
  1. **Baseline rhythm:** Regular intervals based on current baseline frequency ( $\beta(t)$ ), OR
  2. **Stimulus event-driven:** The earliest time when channel importance ( $\alpha_i$ ) exceeds a decaying refractory threshold noise gate. Rings with less intensity cause a lower initial threshold noise gate, allowing for the possibility of high-frequency, faint ringframes.
- **Parallel union sets:** The conscious content of  $[\mathcal{R}, \mathcal{I}]$  may be rendered by a separate, high-frequency  $\mathcal{U}_C$  (content union set) operating in parallel to attention's slower  $\mathcal{U}_A$  (attentional union set). This faint  $\mathcal{U}_C$  could complete multiple refresh cycles (e.g., 3-4 passes in beta/gamma range) within a single  $\mathcal{U}_A$  bin period.

## 1.6 Symbol Glossary

This section defines the mathematical notation used in the Union Set equations for readers unfamiliar with the conventions.

- $\tau$  (tau): The **Ring Period** - the active duration of a sampling cycle.
- $T$ : The **Bin Cycle Period** - the total time from the start of one cycle to the start of the next.  $\tau \leq T$ .
- $\mathbf{x}$ : A point in 3D space,  $\mathbf{x} = (x, y, z)$ .
- $\gamma(t)$ : A **path** or **curve** in space that changes over time,  $t$ .
- $\mathbf{c}(t)$ : The moving center of a shape (e.g., a sphere) along a path.
- $R, R_s$ : Fixed **radii** (sizes) of shapes and their paths.
- $\omega, \omega_s$  (omega): **Angular velocity** - how fast something rotates.
- $\mathbf{p}(\phi)$  or  $\mathbf{p}(s)$ : A **parameterized path**; a way to describe a line or curve using a single parameter (like angle  $\phi$  or distance  $s$ ).
- $\dot{\phi}, \dot{s}$ : The **derivative** (rate of change) of an angle or distance; i.e., the **speed** along the path.
- $\Sigma_k$  (Sigma): A **surface** or boundary captured during the  $k$ -th interrupt.
- $f_k(\mathbf{x}) = 0$ : An **implicit function** defining a surface (all points  $\mathbf{x}$  that satisfy this equation lie on the surface).
- $t_{\text{next}}, t_{\text{last}}$ : The **timestamps** of the next and most recent sampling frames, bin phase  $\phi = 0$ .
- $\beta(t)$  (beta): The dynamic **baseline rhythm** frequency, which wanders between a minimum ( $\beta_{\text{min}}$ ) and maximum ( $\beta_{\text{max}}$ ) value.  $\beta(t)^{-1}$  is the baseline period.
- $\alpha_i$  (alpha): The **salience** or importance of the  $i$ -th external event.
- $\theta(I, \Delta t)$  (theta): The dynamic **triggering threshold**. It depends on the intensity ( $I$ ) of the last frame and the time elapsed ( $\Delta t$ ) since that frame.
- $I_{\text{last}}$ : The **intensity** of the most recent frame.

- $\tau_r$  (tau-r): The **recovery time constant** - controls how quickly the refractory period fades.
- $\theta_\infty, \theta_0$ : The final (resting) and initial **threshold** values.
- $[\mathcal{B}, \mathcal{R}, \mathcal{I}]$ : The domains of the Union Set—**Bank**, **Real**, and **Imaginal** space.
- $\mathcal{T}$ : The target domain (time schema) where information is “printed” or manifested.

## 1.7 Union Set: Integration Framework

The Union Set  $\mathcal{U}$  integrates:

$$\mathcal{U}(t) = \mathcal{B} \cup \mathcal{R} \cup \mathcal{I} \cup \mathcal{T} \quad (10)$$

where  $\mathcal{R}$  = Real Schema,  $\mathcal{I}$  = Imaginal Schema,  $\mathcal{T}$  = Time Schema. The union set is thought to have been observed and noted by Carl Sagan, when he mentioned “outlines of...instant appreciation” [6], and described a similar process of  $[\mathcal{R}, \mathcal{I}]$  magically revealed from  $\mathcal{U}$ .

## 1.8 Bank Skewer: Radial Temporal Gradient

The Bank Skewer  $\mathcal{B}_{\text{Sk}}$  organizes content along a radial temporal gradient within bank space, where present instances interface directly with the Union Set at maximum radius and historical instances decay inward toward the origin. This structure provides simultaneous access to a content type’s complete historical context during ringframe printing.

- **Radial temporal gradient:** Content stacks radially with temporal ordering (present→past),
- **Union Set interface:** Present instances at largest radius directly interact with  $\mathcal{U}$  during sampling,
- **Historical contextualization:** Activation reveals the complete instance history, current content printed against accumulated context,
- **Semantic clustering:** Content types organize along categorical axes within the radial structure.

**Exemplar implementations:**

- **Perceptual events:** Current “specific door opening” printed against hundreds of historical instances,
- **Motor patterns:** Letter ‘b’ writing follows established trajectories through the skewer,
- **Utterance-emotion binding:** Phrases carry accumulated affective weight from historical usage.

The skewer architecture enables efficient recurrent processing through cached pathways while maintaining full historical context for current operations.

## 2 Conscious Representation Mechanism

### 2.1 Processing Hierarchy

Conscious representation follows a strict sequence:

1. **When, How Much, Where:** Temporal indexing by spatial  $\mathcal{B}$  printing ringframe (briefly equaling  $\mathcal{U}$ ) in flowfield  $\mathcal{T}$  at crests in mic  $\mathcal{M}$  ( $\mathcal{M}$  may modulate  $\mathcal{U}$  in phasic mode),
2. **What:** Content binding to  $\mathcal{R}$  and  $\mathcal{I}$ .

## 2.2 Content Determination from Temporal Integration

$\mathcal{R}$  and  $\mathcal{I}$  are deduced from weighted history of  $\mathcal{U}$  (and  $\mathcal{R}$  and  $\mathcal{I}$  when present) in  $\mathcal{T}$ :

$$[\mathcal{R}(t), \mathcal{I}(t)] = f \left( \int_{t-1}^t G(t - \tau) \cdot [\mathcal{U}(\tau), \mathcal{R}(\tau), \mathcal{I}(\tau)] d\tau \right) \quad (11)$$

where  $G$  is half-Gaussian weighting,  $f$  is content deduction function.

### Two Information Streams:

- **Current timing:** Mic level crests compete with a wandering baseline rhythm  $\beta(t)$  to trigger new ringframe printings (briefly equal  $\mathcal{U}$ ),
- **Content determination:** Weighted history determines  $[\mathcal{R}(t), \mathcal{I}(t)]$ .

## 3 Discussion

### 3.1 Binding Problem Resolution

RBT provides geometric solutions:

- **Spatial unity:** Shared  $\mathcal{U}$  coordinates,
- **Temporal flow:** Overlapping access windows in  $\mathcal{T}$ ,
- **Qualia:** Emergent properties of access kinematics.

### 3.2 Connection to Peircean Semiotics

Consciousness operates through cascading semiotic stages, where the interpretant of one stage becomes the representamen of the next:

- **Stage 1 (Perceptual):** A crafted **mic+baseline signal** (Representamen) is interpreted into **Union Set ringframes** (Interpretant), which serves as the initial perceptual **Object**,
- **Stage 2 (Cognitive):** This perceptual ringframe-Object then becomes the new **Representamen**, which, combined with the ongoing signal, is interpreted into a full **Real+Imaginal schema** (Interpretant) — the understood world-situation as the new **Object**,
- **Stage 3 (Metacognitive):** This R+I situation-Object becomes the final **Representamen**, interpreted for **threats/affordances** (Interpretant) that directly drive **behavioral output** (Object).

### 3.3 Neural Correlates: Hyperpolarization and Conscious Access

Hyperpolarization dynamics may shape Union Set phenomenology across the phasic-to-interrupt continuum:

- **Semiotic modulation:** Hyperpolarization increases latency of meaning-making, impacting both phasic and interrupt modes,
- **Potential ensemble broadening:** Rhythmic inhibition may engage larger-than-typical neural populations, possibly explaining enhanced bank visibility,
- **Global entrainment:** HCN1 channels in layer 5 pyramidal neurons (in retrosplenial cortex) coordinate cortex-wide rhythms during hyperpolarization,

- **Baseline rhythm generation:** The wandering baseline  $\beta(t)$  may originate from retrosplenial/DMN activity, phase-locking to high-level mic events including interoceptive signals such as heartbeats. Both salient events and intrinsic oscillations contribute to pulse generation, with the  $\sim 2$  Hz rhythm comprising nested  $\sim 80$  Hz bursts followed by  $\sim 450$  ms of refractory silence.

Hyperpolarization may enhance conscious sampling along the access gradient by increasing semiotic latency and potentially recruiting beyond specific sparse ensembles (entire  $\mathcal{B}$  rather than just the  $\mathcal{U}$  manifold) [1, 2]. Vesuna et al. demonstrated that HCN1 channels in rat retrosplenial cortex layer 5 (analogous to human default mode network) generate the 2 Hz rhythms during ketamine hyperpolarization. Out-of-phase bursting between regions may transiently functionally disconnect them, potentially underlying dissociation [3].

### 3.4 Photic Entrainment: Modality-Specific Sampling Modulation

Rhythmic photic stimulation entrains faint Union Set sampling with distinct characteristics from hyperpolarization-driven states:

- **Modality-specific entrainment:** Visual sampling synchronizes to external rhythms while other modalities maintain independent timing,
- **Reduced embodiment:** Lacking global (and local) hyperpolarization, entrained sampling remains localized without cross-modal broadcast, and does not affect meaning-making rates of visual or other cortical areas,
- **Preserved parallel processing:** Gamma-range events continue uninterrupted in non-entrained modalities.

Unlike hyperpolarization states that create global bottlenecks and cross-modal integration, photic entrainment demonstrates that sampling rhythms can be selectively modulated within specific sensory channels while preserving parallel processing capacity across the system.

### 3.5 FM-PCA Rings: Motor and Temporal Processing

Neural correlates of rhythmic processing demonstrate ring-like dynamics in motor and premotor cortices:

- **Motor cortex rings:** Frequency-modulated PCA trajectories in monkey motor cortex ( $\sim 1\text{--}3$  Hz) phase-lock to cyclic behaviors like hand pedaling, providing a neural basis for ring-like processing during rhythmic movement [4],
- **Temporal processing rings:** Medial premotor cortex exhibits similar ring dynamics ( $\sim 1\text{--}2$  Hz) that align with both external and internal tempo tasks, with  $0^\circ$  phase correlating with beat onset [5].

These neural ring dynamics share frequency-locking characteristics with phenomenal ringframes observed during rhythmic perception and action, suggesting conserved computational principles for temporal processing across neural and phenomenal domains.

### 3.6 Neural Correlates: Union Set Activation

The active phase of  $\mathcal{U}$ , particularly during interrupt-mode sampling, may correspond to specific neural dynamics. Ketamine studies suggest a potential correlate in 80 Hz cortical bursts nested within  $\sim 2$  Hz rhythms from retrosplenial/default mode network regions, though this mapping



requires finer temporal resolution. Initial EEG evidence indicates beta/gamma power fluctuations in medial prefrontal cortex coincided with expected  $\mathcal{U}$  activation to musical transients [7]. Additional candidate mechanisms include rhythmic inhibitory pulses from the thalamic reticular nucleus, thalamic matrix cell coordination, Pulvinar responses, and hippocampal theta oscillations. Alternatively, parallel instantiations of  $\mathcal{U}$  may exist across brain regions during normal levels of polarization, with individual regions rallying around local burst timing. MIT’s Earl Miller found frequency chirps (max power cycling from 2 to 80 Hz) chunked into repeating 2 Hz bins, potentially correlating to a phasic or gross-to-fine mode of  $\mathcal{U}$  behavior [8]. Steven Lehar (on page 91 of his book, “Grand Illusion”) mentions cyclic frequency chirps rendering gross-to-fine scale geometry of  $\mathcal{R}$  [10], indicating a progressive enhancement of semiosis within each processing bin, possibly indicating that perceptual color is a final or later step in semiosis. The gist of necessary meaning can be obtained from geometry alone, prior to addition of color, as evidenced by movies in black-and-white. His drawings on page 93 appear to depict  $\mathcal{B}$  and possibly  $\mathcal{T}$ . Lehar’s work is explored in greater depth by Cube Flipper [11].

## Conclusion

Ring Bank Theory proposes that conscious orchestration (in hyperpolarized state) involves:

1. A high-level **microphone** signal  $\mathcal{M}$  whose crests compete with a sometimes-present **baseline rhythm**  $\beta(t)$  to trigger interpretation into **ringframes** and  $[\mathcal{R}, \mathcal{I}]$  schemas,
2. A **bank** ( $\mathcal{B}$ ) maintaining perspective-invariant space, with rare **skewers** ( $\mathcal{B}_{\text{Sk}}$ ) for radial temporal stacking,
3. **Real and imaginal schemas**  $[\mathcal{R}, \mathcal{I}]$  rendering world-model and non-veridical content from  $[\mathcal{M}, \mathcal{U}, \mathcal{B}]$  with characteristic latency from events and extrapolative prediction into expected present (as possible),
4. A **time schema**  $\mathcal{T}$  flowfield, with a fading history of (once-**union set**) **ringframes**,
5. A **union set** ( $\mathcal{U}$ ), operating with a gradient from continuous-to-discrete (phasic-to-interrupt), integrating spatial, real, imaginal, and temporal schemas;  $\mathcal{R}$  and  $\mathcal{I}$  may lag  $\mathcal{M}$ ,  $\mathcal{U}$  and  $\mathcal{B}$ ,
6. And a **body schema**, within real  $\mathcal{R}$ , servo-linked to drive physical body.

## References

- [1] Caldwell, B. B. (2022). *Rings of Fire: How the Brain Makes Consciousness*.
- [2] Caldwell, B. B. (2023). *Perceptual Optics*.
- [3] Vesuna, S. et al. (2020). Deep posteromedial cortical rhythm in dissociation. *Nature*.
- [4] Saxena, S., Russo, A. A., Cunningham, J., & Churchland, M. M. (2022). Motor cortex activity across movement speeds is predicted by network-level strategies for generating muscle activity. *Neuron*, 110(5), 839-855.
- [5] Gámez, J., Mendoza, G., Prado, L., Betancourt, A., & Merchant, H. (2019). The amplitude in periodic neural state trajectories underlies the tempo of rhythmic tapping. *PLOS Biology*, 17(5), e3000054.
- [6] Sagan, Carl. (n.d.). *Mr. X. Organism Earth*. Retrieved from <https://www.organism.earth/library/document/mr-x>.



- [7] Caldwell, Brad. (2025). *Spectral Amplitude Modulation in EEG: Potential Correlations with Musical Stimuli*. Figshare. DOI: 10.6084/m9.figshare.27115354. <https://nodes.descri.com/dpid/419/v1>.
- [8] Adam, E., Kowalski, M., Akeju, O., Miller, E. K., Brown, E. N., McCarthy, M. M., & Kopell, N. (2024). Ketamine can produce oscillatory dynamics by engaging mechanisms dependent on the kinetics of NMDA receptors. *Proceedings of the National Academy of Sciences*, 121(22), e2402732121. <https://doi.org/10.1073/pnas.2402732121>.
- [9] Lehar, Steven. (2008). *The Constructive Aspect of Visual Perception: A Gestalt Field Theory Principle of Visual Reification Suggests a Phase Conjugate Mirror Principle of Perceptual Computation*. slehar.com. <http://slehar.com/www/ConstructiveAspect/ConstructiveAspect.html>.
- [10] Lehar, Steven. (2010). *The Grand Illusion: A Psychonautical Odyssey into the Depths of Human Experience*. slehar.com. <http://slehar.com/wwwRel/GrandIllusion.pdf>.
- [11] Cube Flipper. (2022, November 22). *An introduction to Steven Lehar, part II: Symmetries and periodicities*. Smooth Brains. <https://smoothbrains.net/posts/2022-11-22-an-introduction-to-steven-lehar-part-ii.html>
- [12] Ronnie\_Yonk. *[3D Model of Cobain and Stage]*. Cults. Retrieved [2022], from cults3D.com.
- [13] GIGI\_TOYS. *[3D Model of Driver/Wheel]*. Cults. Retrieved [2022], from cults3D.com.

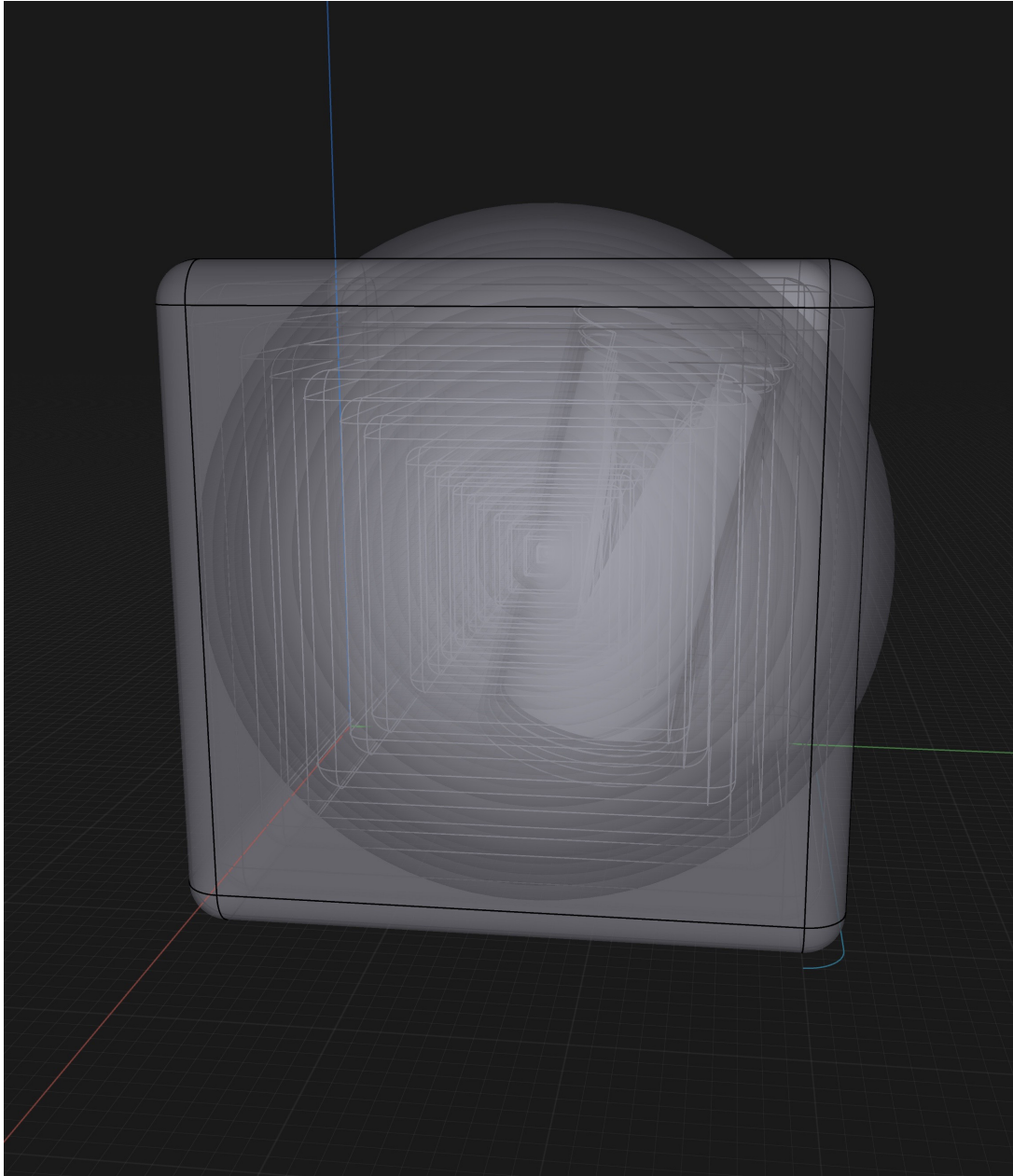


Figure 1: Depiction of the Bank Schema ( $\mathcal{B}$ )

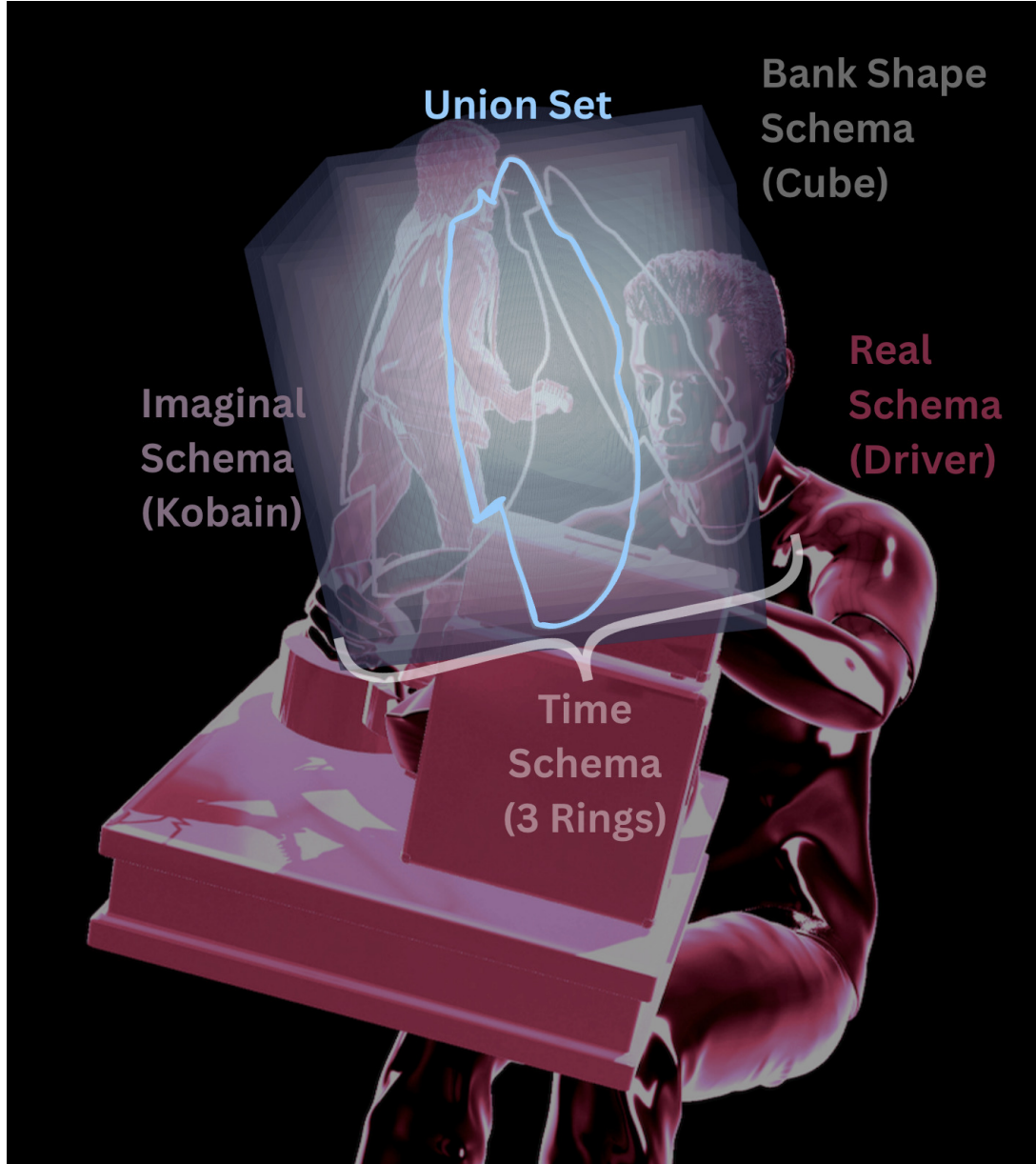


Figure 2: Union Set  $\mathcal{U}$  (of  $\mathcal{B}$ ,  $\mathcal{R}$ ,  $\mathcal{I}$  and  $\mathcal{T}$ ); the models were sourced from online creators [12, 13]

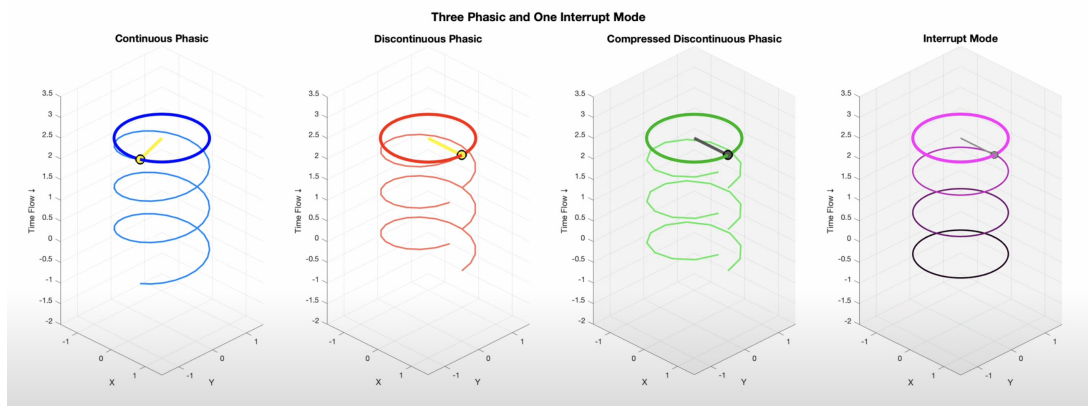


Figure 3: Fusing Gradient: Phasic Mode to Interrupt Mode (of  $\mathcal{U}$  in  $\mathcal{T}$ )